This paper appears in IET Control Theory & Applications, vol. 8, no. 17, pp. 1769-1780, 2014.
http://dx.doi.org/10.1049/iet-cta.2013.0908

Stability of Sampled-Data, Delayed Haptic Interaction under Passive or Active Operator

Noushin Miandashti* Mahdi Tavakoli, IEEE Member†

Department of Electrical and Computer Engineering, University of Alberta, Edmonton, AB T6G 2V4, Canada

Abstract

This paper studies the absolute stability of a sampled-data, m-user haptic virtual environment (HVE) system based on the discrete-time circle criterion. Depending on the task being performed by an operator, the passivity of the operator is influenced. We provide a framework for the system stability analysis in which the operator is allowed to exhibit passive or active behavior. In this paper, the well-known Colgate's stability condition for a 1-user haptic system with a passive operator is reproduced and then extended to the m-user case while allowing each or all of the operators to behave passively or actively. Another extension to Colgate's condition comes by allowing communication delays to exist in the system. Simulations and experiments confirm the validity of the proposed conditions for stability of sampled-data, delayed m-user HVE systems.

1 Introduction

A haptic interface acts as a link between a human operator and a virtual environment and conveys a kinesthetic sense of presence in the virtual environment to the operator. The combined system is *sampled-data* as it includes a virtual environment simulated in a digital computer and a human operator and a haptic interface that are actual physical systems. For this system, stability is a prime concern because it may be jeopardized by the discrete-time simulation of the virtual environment due to its inherent sampling effects.

Investigations done on energy leaks caused by the sample-and-hold in sampled-data haptic interaction has shown that a zero-order-hold (ZOH) accounts for a half-sample delay and has energy-instilling effects [1]. To qualitatively explain this, consider haptic interaction with a finite-impedance virtual object where the interaction forces are sampled and fed back to the user. As the virtual object is penetrated by the virtual tool, the sampled forces will be less than the real forces during each sampling intervals, resulting in the forces reflected to the user to be too low. By contrast, as the virtual tool moves out of the object, the reflected forces will be too high compared to reality. Thus, the user's legitimate expectation that a passive object would not generate energy is violated. Indeed, as the user utilizes the haptic device to probe the virtual object by pushing and letting go of the user interface, the energy-instilling sampled-data coupling presents the object to the user as one emitting energy and causing vibrations, an effect never observed when touching the same object directly by hand.

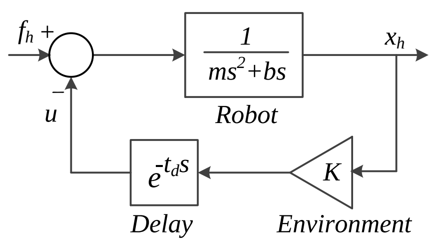

Figure 1: A continuous model for a single-user HVE system

A number of authors have considered the issue of stability in sampled-data haptic interaction in the virtual space. Minsky et al. [2] were the first to study this problem. As shown in Figure 1, they considered a continuous-time model of a one degree-of-freedom (DOF) haptic device interacting with a discretely-simulated virtual wall. The robot (haptic interface) was modeled as a mass m and a damping b connected to the virtual wall by a virtual coupling (digital controller) modeled by a stiffness K. In their study, system instabilities were attributed to the time delay introduced by the hold operation; in fact, the hold operation is absent from Figure 1 because it was replaced by a time delay t_d of one sampling period T approximated by a second-order Taylor series expansion.

It was shown that the system in Figure 1 is stable if

$$b > KT \tag{1}$$

*e-mail: miandash@ualberta.ca
†e-mail: mahdi.tavakoli@ualberta.ca

They argued that the above condition is approximate and in reality there is a constant C approximately equal to $1/2$ for which $b > C * KT$ is the true stability condition. Also, they showed via experiments that with the operator's mass m_h, damping b_h and stiffness k_h, and with a virtual damping B complementing the virtual stiffness K, the stability condition will become

$$B + b + b_h > \frac{(K + k_h)T}{2} \quad (2)$$

A more rigorous examination of stability was performed by Colgate and Schenkel [3]. They again considered a 1-DOF haptic interface to derive necessary and sufficient conditions under which a sampled-data haptic display system would exhibit passive behavior. For a common discrete-time implementation of the virtual environment composed of a spring and a damper in parallel as in Figure 2, which is essentially a discrete-time PD controller, the necessary and sufficient condition for passivity and absolute stability[1] of the sampled-data HVE system was derived as

$$b > \frac{KT}{2} + B \quad (3)$$

This result shows that some physical dissipation in the haptic interface (i.e., $b > 0$) is essential to achieving passivity and absolute stability. On the other hand, high robot damping causes poor performance. The upper limit on the environment stiffness imposed by the stability condition implies that in order to implement a highly stiff, dissipative wall constraint, it is imperative to lower the sampling period T as much as possible.

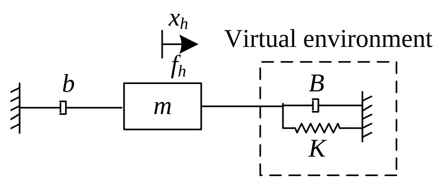

Figure 2: The physical model for a single-user HVE system

Another approach to the stability analysis of a similar HVE system was provided by Gil et al. In [4], using the Routh-Hurwitz criterion, the closed-loop stability problem of the 1-DOF HVE system was addressed directly; this is distinct from the absolute stability and passivity analysis in [3]. The environment was modeled as a virtual spring and damper in mechanical parallel and the stability condition was derived as

$$b + B > \frac{KT}{2} \quad (4)$$

The above condition was shown to be valid only for low values of the virtual damping B. Comparing Colgate's and Gil's condition, it is easily seen that the passivity criterion is more conservative than the stability criterion. As for the human operator model, it has been argued in [4], [5] and [6] that the operator only contributes positively to stability (i.e., the absence of a user amounts to a worst-case scenario for stability) as long as it is passive, thus the operator effect is neglected in the stability analysis; note that the operator is simply modeled as an external input force f_h. However, as mentioned later, passivity of the operator is case-dependent and that is why that in this paper we will introduce a new method that will allow us to account for active operators as well.

The stability of time-delayed HVE systems has been inspected in [7], once again assuming that the operator is passive and that the virtual damping B is small. For a delay t_d, which can be the sum of several effects (computations, communications, etc), the stability condition was found to be

$$K < \frac{B + b}{T + t_d} \quad (5)$$

The passivity of the operator is simply a convenient assumption used in all of the above work for stability analysis of a haptic system independent of the typically uncertain, time-varying and/or unknown dynamics of the operator. However, given that the operator voluntarily manipulates the master robot and thereby has the capacity to inject energy into the system, this assumption may not always be valid depending on the task. Active behavior of the operator in a haptic system has been reported in [8].

In this paper, a discrete-time circle criterion based framework to find the stability condition for a sampled-data, delayed haptic system in the presence of passive or active operator is proposed. While in the context of stability analysis of feedback systems, Lur's function and the circle and Popov criteria have been used in the continuous-time domain [9, 10], using the discrete-time circle criteria in studying the stability of sampled-data HVE and teleoperation systems is a new topic. This paper derives Colgate's stability condition for a passive operator in a new and simplified way and extends it to the case of an active operator. Also, while because of the nature of Colgate's or Gil's methods, it is difficult to extend them to multiple-operator collaborative HVE systems, our proposed method is easily extended to the m-user case where $m \geq 2$.

Many applications of multi-user collaborative HVEs in surgical training [11, 12], telerehabilitation [13, 14, 15], gaming [16, 17], etc. have been reported in literature. This paper studies the stability of multi-user HVEs based on the client-server architecture. When considering

[1]Since the human operator model is unknown, there is interest in absolute stability and passivity methods instead of conventional stability method. A common assumption in absolute stability and passivity methods is that the operator behaves passively.

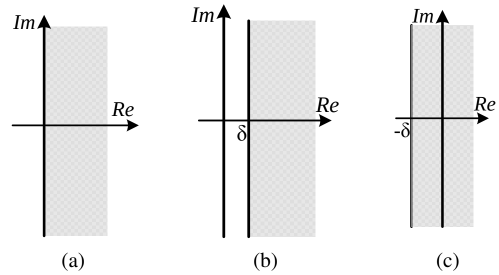

Figure 3: Nyquist diagrams of (a) a passive system, (b) an *ISP* system with excess of passivity of δ, (c) an active system with shortage of passivity of δ

client-server architecture, we should also account for the transmission delay of the visual and haptic commands. With this another extension to Colgate's stability condition comes by allowing communication delays to exist in the system.

The rest of the paper is organized as follows. Section 2 provides mathematical preliminaries required for the rest of the paper. Section 3 is divided into two subsections 3.1 and 3.2. In Section 3.1, for the single-user haptic system in Figure 4a, stability conditions for both passive and active operators as well as under delayed or non-delayed channels are derived. In Section 3.2, a model for a sampled-data, *m*-user collaborative HVE is proposed and its stability conditions are derived. In Section 4, the simulation results are described. Experimental results are presented in Section 5 and Section 6 presents the conclusions.

2 Mathematical Preliminaries

Definition 1. *[18] The memory-less system*

$$y = h(t,u)$$

is passive if

$$u^T y \geq 0$$

Otherwise, it is active.

Lemma 1. *[18] The LTI minimal realization*

$$x(i+1) = Ax(i) + Bu(i) \quad (6)$$

$$y(i) = Cx(i) + Du(i) \quad (7)$$

with $G(z) = C(zI - A)^{-1}B + D$ is

- *passive if $G(z)$ is positive real;*
- *strictly passive if $G(z)$ is strictly positive real.*

Definition 2. *[18] An $m \times m$ proper rational transfer function matrix $G(z)$ is positive real if*

- *poles of all elements of $G(z)$ are inside or on the unit circle*
- *for all real ω for which $e^{j\omega}$ is not a pole of any element of $G(z)$, the matrix $G(e^{j\omega}) + G^T(e^{-j\omega})$ is positive semidefinite, and*
- *the poles of any element of $G(z)$ on $|z| = 1$ are simple and the associated residue matrices of these poles are positive semidefinite.*

Definition 3. *[18] Let A be a Hermitian symmetric matrix. A is positive semidefinite, if all its leading principle minors are non-negative. A is positive definite if all its leading principle minors are positive.*

Definition 4. *Consider a system with input $u(t)$ and output $y(t)$. If there exists constant a β such that for all $t \geq 0$,*

$$\int_0^t y(\tau)u(\tau)d\tau \geq \beta \pm \delta \int_0^t u(\tau)u(\tau)d\tau \quad (8)$$

then for $\delta > 0$ the system is input strictly passive (ISP) with excess of passivity (EOP) [19] of (at most) δ if equation (8) holds the plus sign [20]. For the same $\delta > 0$, the system is active with shortage of passivity (SOP) of (at most) δ if the equation (8) has minus sign.

Passivity of an LTI system is equivalent to having the system's Nyquist diagram entirely in the right half plane (Figure 3a). The Nyquist diagram of an ISP system with transfer function $G(s)$ and EOP of $\delta > 0$ is in the right hand side of the vertical line at δ, i.e. $\Re G(s) \geq \delta$ (Figure 3b). Similarly, for a non-passive transfer function $G(s)$ with SOP of $\delta > 0$ the Nyquist diagram is in $\Re G(s) \geq -\delta$ (Figure 3c).

Theorem 2.1. *[21] Consider a sampled-data multivariable control system that consists of an LTI system $G(s)$ in the forward path and the nonlinearity $\phi = \phi(y)$ in the feedback path. Such a system can be presented by the difference equation*

$$x(i+1) = Ax(i) - B\phi(y) \tag{9}$$

$$y(i) = Cx(i),\ \ y \in R^m \tag{10}$$

$$\phi(y) = [\phi_1(y_1), \phi_2(y_2), ..., \phi_m(y_m)]^T \tag{11}$$

If there exists $K = diag(k_1, ..., k_m) > 0$ such that

$$K^{-1} + C(zI - A)^{-1}B \tag{12}$$

is positive real then $G(z)$ is absolutely stable for any ϕ satisfying

$$\phi(0) = 0,\ 0 < y_i\phi(y_i) \leq y_i^2 k_i, \quad y_i \neq 0 \tag{13}$$

Thus, the sampled-data system (9)-(11) will be stable. For a passive ϕ, $k_i \to \infty$ and condition (12) will change to $G(z)$ being positive real.

3 STABILITY ANALYSIS OF HAPTIC VIRTUAL ENVIRONMENTS

This section comprises of two subsections. In Section 3.1, the stability of the single-user 1-DOF HVE system in Figure 2 is studied. When there is no delay, Colgate's stability condition is arrived at using the proposed framework and based on the discrete-time circle criterion in Theorem 2.1. Also, the stability condition in the presence of delay is derived. In both cases, the effect of an active operator on the stability condition is studied. Later in Section 3.2, a multi-user 1-DOF HVE system is considered and for both non-delayed and delayed cases the stability condition is derived while accounting for possible operator activity.

3.1 A Sampled-Data Single-User HVE System

In this section two methods for stability analysis of single-user HVE systems are provided. The first method is based on discrete-time circle criterion and is the proposed method in this paper and is explained in Section 3.1.1. In Section 3.1.2 the previously proposed method in [3] is extended to the cases where the communication time-delay can exist in the system while the operator is allowed to behave actively. It is shown that both methods result in the same stability conditions for single-user HVE systems.

3.1.1 Discrete-Time Circle Criterion Based Method

The block diagram of the single-user HVE system in Figure 2 is shown in Figure 4a, where $Z_h(s)$ is the unknown human operator model and $H(z)$ is the known discrete-time model of the environment (i.e., the digitally-implemented virtual coupling between the haptic interface and the virtual wall). As before, the haptic interface is a rigid manipulator and is modeled as a mass m and a damper b. The input and output of $H(z)$ pass through a sampler and a ZOH with a sampling period of T, respectively. Simple manipulations in the block diagram in Figure 4a will result in the one in Figure 4b. The equations governing the resulting system in Figure 4b will be

$$f_h - u = bv_h \tag{14}$$

$$x_h = \frac{v_h}{s} \tag{15}$$

$$u^* = z^{-n}H(z)x_h^* \tag{16}$$

With the assumption that $n = t_d/T$ is an integer (t_d represents the communication delay), the discrete-time equivalent of (14) is

$$f_h^* - u^* = bv_h^*$$

and with the help of (16) we get

$$f^* - z^{-n}H(z)x_h^* = bv_h^*$$

The above can be written in the z-domain as

$$F(z) - z^{-n}H(z)X_h(z) = bV_h(z)$$

where

$$X_h(z) = \mathscr{Z}\{\frac{v_h}{s}\}$$

It is important to note that $\mathscr{Z}\{\frac{v_h}{s}\} \neq \mathscr{Z}\{\frac{1}{s}\}V_h(z)$ [6]. To be able to derive the transfer function from f_h to v_h, we need to approximate $\mathscr{Z}\{\frac{v_h}{s}\}$. We can do so based on one of the following approximation methods:

- Forward Difference

$$x_h(kT+K) = x_h(kT) + T\dot{x}_h(kT) \xrightarrow{\mathscr{Z}} zX_h(z) = X_h(z) + TV_h(z)$$
$$\Longrightarrow X_h(z) = \frac{T}{z-1}V_h(z)$$

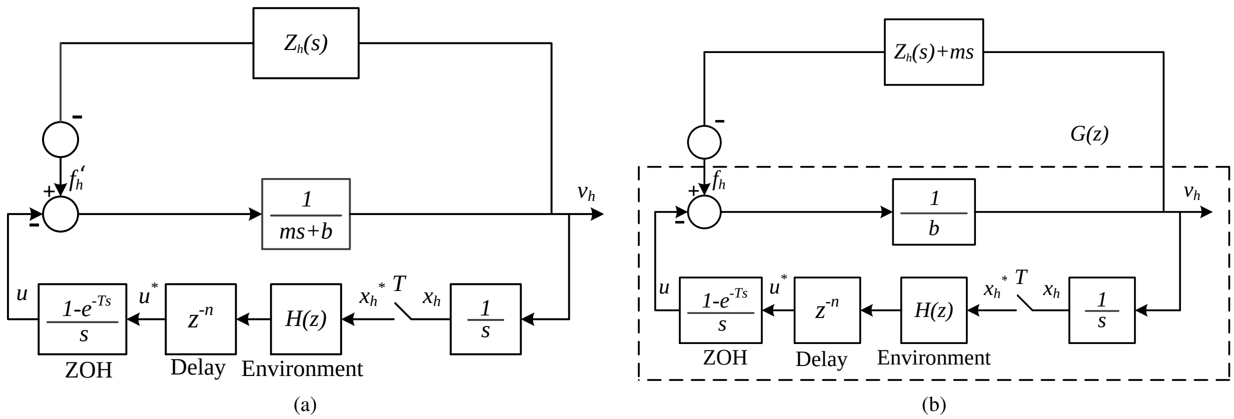

Figure 4: Model of a 1-DoF sampled-data HVE system

- Backward Difference

$$x_h(kT) = x_h(KT-T) + T\dot{x_h}(kT) \xrightarrow{\mathscr{Z}} X_h(z) = z^{-1}X_h(z) + TV_h(z)$$
$$\Longrightarrow X_h(z) = \tfrac{Tz}{z-1}V_h(z)$$

- Tustins Transformation

$$x_h(kT+T) = x_h(kT) + T\dot{x_h}(kT) + (\dot{x_h}(kT+T) - \dot{x_h}(kT))\tfrac{T}{2}$$
$$\xrightarrow{\mathscr{Z}} zX_h(z) = X_h(z) + TV_h(z) + (zV_h(z) - V_h(z))\tfrac{T}{2}$$
$$\Longrightarrow X_h(z) = \tfrac{T}{2}\tfrac{z+1}{z-1}V_h(z)$$

In previous related works [3, 22, 5, 7] the impedance of the environment in the z domain has been approximated as $H(z) = K + \frac{B(z-1)}{Tz}$ and, we will use the same model. In the following, we consider four cases for operator passivity and communication delay.

Passive Operator, No Delay Assuming that $t_d = 0$, depending on which approximation is chosen, the f to v mapping will be one of the following:

$$F_h(z) = bV_h(z) + (K + \frac{B(z-1)}{Tz})\frac{T}{z-1}V_h(z) = G_1^{-1}(z)V_h(z)$$
$$F_h(z) = bV_h(z) + (K + \frac{B(z-1)}{Tz})\frac{Tz}{z-1}V_h(z) = G_2^{-1}(z)V_h(z)$$
$$F_h(z) = bV_h(z) + (K + \frac{B(z-1)}{Tz})\frac{T}{2}\frac{z+1}{z-1}V_h(z) = G_3^{-1}(z)V_h(z)$$

The above correspond to forward difference, backward difference and Tustin approximations, respectively. Based on Theorem 2.1 for $m = 1$, since $Z_h(s) + ms$ is passive, the system in Figure 4b is stable if $G(z)$ is positive real. Based on Lemma 1 and using the fact that passivity of $G(z)$ is equal to $G^{-1}(z)$ being passive [23], the stability of the system is ensured if $G^{-1}(z)$ is positive real. The first condition for positive realness of $G^{-1}(z)$ is satisfied since it can be clearly seen that the poles of $G_i^{-1}(z)$, $i = 1,2,3$, lie inside or on the unit circle. Since $z = 1$ is a simple pole and its residue for each $G_i^{-1}(z)$ is positive semidefinite, KT, the only remaining condition to check is the second condition in the Definition 2, which for $m = 1$ will reduce to $\Re\{G_i^{-1}(z)\} \geq 0$. In this way, the conditions for stability of the single-user HVE system based on the three approximations are found as follows:

$$b > \frac{KT}{2} - B\cos(\omega T) \tag{17}$$
$$b + \frac{KT}{2} + B > 0 \tag{18}$$
$$b + B\frac{1+\cos(\omega T)}{2} \tag{19}$$

From (17)-(19), the worst-case condition is (17). In turn, (17) assumes its worst-case $\cos(\omega T = -1$, when we will have

$$b > \frac{KT}{2} + B \tag{20}$$

This is identical to Colgate's condition. As shown, forward difference approximation method resulted in the worst-case condition for stability of the single-user HVE system. As a result, in the rest of the paper, the $\frac{1}{s}$ is approximated using the forward difference approximation method.

Passive Operator, Delay The previous condition was found assuming no delay in the system. For a delayed single-user HVE system, the stability condition will take a different form depending on the virtual environment model. Here again, it can be shown that forward difference approximation method for $\frac{1}{s}$ will lead us to the worst-case condition. The f to v mapping in the z domain will then be

$$F_h(z) = bV_h(z) + z^{-n}(K + \frac{B(z-1)}{Tz})\frac{T}{z-1}V_h(z) \tag{21}$$

Since the passivity of $G(z)$ is equal to $G^{-1}(z)$ being passive, the delayed sampled-data HVE system is stable if (22) is positive real:

$$G^{-1}(z) = b + z^{-n}(K + \frac{B(z-1)}{Tz})\frac{T}{z-1} \tag{22}$$

The first and third conditions in Definition 2 are readily satisfied leaving us with the third condition which requires $\Re\{G^{-1}(z)\} \geq 0$. Substituting $z = \cos(\omega T) + j\sin(\omega T)$ in (22) the real part of $G(j\omega)^{-1}$ must satisfy:

$$b + B\cos(\omega t_d - T) - \frac{KT}{2}\cos(\omega t_d) - KTS > 0 \tag{23}$$

where, $S = \frac{\sin(\omega t_d)\sin(\omega T)}{2(1-\cos(\omega T))}$. With the assumption that $t_d/T = n$ and B is small, the worst-case condition will happen if $\cos(\omega T) = 1$. Then, we have

$$\lim_{\cos(\omega T)\to 1} KTS = \lim_{\cos(\omega T)\to 1} KT\frac{\sin(\omega t_d)\sin(\omega T)}{2(1-\cos(\omega T))} = Kt_d$$

and (23) will simplify to

$$b + B - \frac{KT}{2} - t_d/T\cos(\omega T/2) > 0 \tag{24}$$

For $\cos(\omega T/2) = 1$ the passivity condition for a delayed single-user HVE system will be derived as follows:

$$b + B > \frac{KT}{2} + Kt_d \tag{25}$$

Interestingly, the above condition is identical to the condition reported in [7].

Active Operator, No Delay The same approach will also enable us to inspect the stability of sampled-data HVE systems with an active operator. Note that previously in Figure 4b, in order to simplify the system, the mass m of the master device was moved to the operator impedance $Z_h(s)$ without affecting the overall system or the passivity of the new operator $Z_h(s) + ms$. Now, employing a similar technique, given that we want to allow the operator to be active, we will move enough of damping b of the master device to the operator impedance $Z_h(s)$ to render it passive. Let's name the real part of the operator impedance Z_h to be $-z_a$. When $z_a > 0$, it represents the shortage of passivity of an active operator. Let us transfer z_a units of the master device damping b, to $Z_h(s)$ to neutralize this shortage of passivity and make the new operator passive. As a result, based on (20) and after replacing b by $b - z_a$, the stability condition after accounting for the active operator effect will be

$$b - z_a > \frac{KT}{2} + B \tag{26}$$

Evidently, the proposed condition (27) extends the condition in [3] by both allowing the operator to be active and for the delay to exist, and extends the condition in [7] by allowing the operator to be active. The above shows an inevitable trade-off faced when allowing for active operators. Although higher robot dampings go against conventional wisdom due to the associated performance degradations, we see that it is the price to be paid for allowing active intervention of the operators.

Active Operator, Delay In the case of a delayed HVE system in which the operator has shortage of passivity of z_a, again the approach is the same as for active operator without delay. We will transfer z_a units of the master device damping b, to $Z_h(s)$ to neutralize the shortage of passivity and make the new operator passive. Based on (25) and after replacing b by $b - z_a$, the stability condition for a delayed single-user HVE system with active operator will be

$$b - z_a + B > Kt_d + \frac{KT}{2} \tag{27}$$

3.1.2 Small-Gain Theorem Approach

The above results, which were derived using the proposed simplified framework, can also be derived using the method in [3], which did not allow for the operator to be passive or for a delay to exist. This extension constitutes another contribution of this paper.

The closed-loop characteristic equation of the sampled-data HVE system in Fig. 4a is $1 + H(e^{sT})G_T{}^*(s) = 0$ where $G_T{}^*(s) = \frac{1}{T}\Sigma_{k=-\infty}^{\infty} G_T(s + jk\omega_s)$ and $G_T(s) = \frac{1-e^{-Ts}}{s^2}\frac{1}{ms+b+Z_h(s)}$. Note that the feedback interconnection of $\frac{1}{ms+b}$ and $Z_h(s)$ results in $\frac{1}{ms+b+Z_h(s)}$.

In order to understand the following analysis, Figure 5 is key. The human operator with impedance Z_h in Figure 5a is allowed to be active with a shortage of passivity equal to $z_a \geq 0$. In Figure 5b, this impedance is shifted to the right by b (it is assumed that $b > z_a$). It is easy

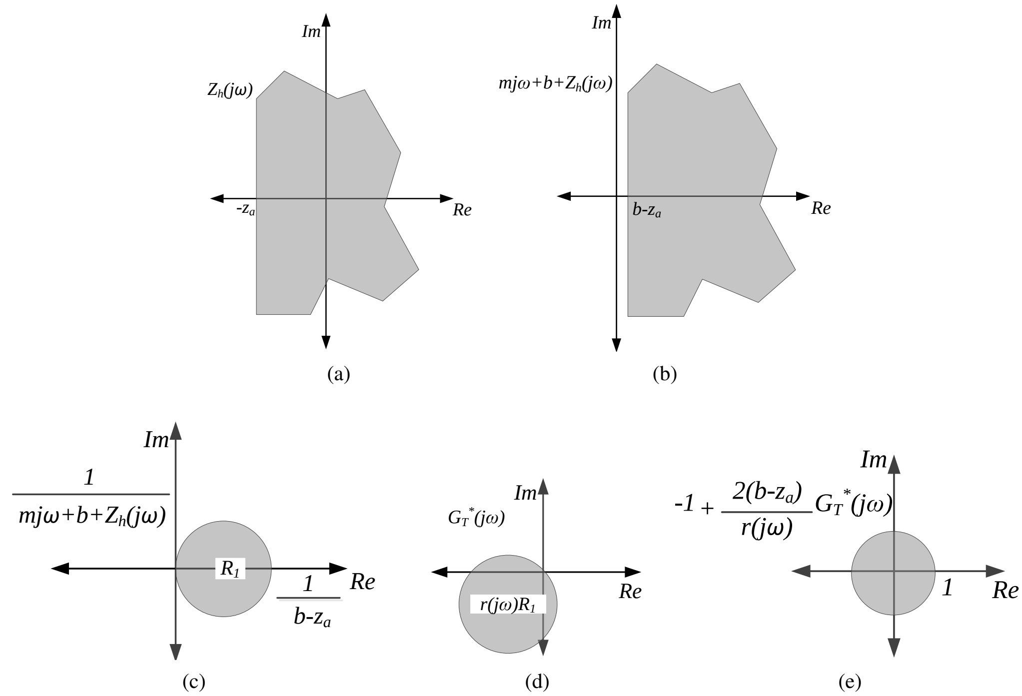

Figure 5: The Nyquist plots of (a) operator impedance with shortage of passivity of z_a, (b) the inverse closed-loop transfer function of the operator and robot impedances, (c) the closed-loop transfer function of the operator and robot impedances, (d) $G_T{}^*(s)$ and (e) the mapping of $G_T{}^*(s)$ into the unit circle.

to see that the feedback interconnection of the operator impedance Z_h and the robot impedance $\frac{1}{ms+b}$ will span the complex plane region R_1 shown in Figure 5c. In a manner similar to [3], it can be shown that $G_T{}^*(s)$ covers the region $R_{G_T{}^*}(\omega) = r(j\omega)R_1$ shown in Figure 5d, where

$$r(j\omega) = e^{-j\omega t_d}\frac{T}{2}\frac{e^{-j\omega T}-1}{1-\cos(\omega T)} \tag{28}$$

once we assume that t_d is an integer multiple of T.

Theorem 3.1. *The sampled-data system in Figure 4a will be stable if*

$$\|\mathscr{M}\mathscr{N}\|_\infty < 1 \tag{29}$$

where $\mathscr{M}$ and $\mathscr{N}$ are linear fractional tranformations defined as

$$\mathscr{M}\{s, G_T{}^*(s)\} = -1 + \frac{2(b-z_a)}{r(s)}G_T{}^*(s) \tag{30}$$

$$\mathscr{N}\{s, G_T{}^*(s)\} = \frac{r(s)H(e^{sT})}{2(b-z_a)+r(s)H(s))} \tag{31}$$

Proof. For the absolute stability of a single-user HVE system in Figure 4a, it is necessary and sufficient that the closed-loop characteristic equation of the system $(1+H(e^{sT})G_T{}^*(s)=0)$ has all of its roots in the left half of the complex plane. Let us find $\mathscr{M}$ and $\mathscr{N}$ can be found such that the transformed characteristic equation

$$1+\mathscr{M}\mathscr{N} = 0 \tag{32}$$

has the same roots as the original characteristic equation of the sample-data single-user HVE system $1+H(e^{sT})G_T{}^*(s)=0$. As it can be seen in Figure 5e, the appropriate linear fractional transformation applied to $G_T{}^*(s)$ that will provide the appropriate translation and scaling to map $R_{G_T{}^*}(\omega)$ to the unit disk in Figure 5e will be

$$\mathscr{M}\{s, G_T{}^*(s)\} = -1 + \frac{2(b-z_a)}{r(s)}G_T{}^*(s) \tag{33}$$

By replacing $\mathscr{M}$ in (32) and comparing with $1+H(e^{sT})G_T{}^*(s)=0$, $\mathscr{N}$ will be

$$\mathscr{N}\{s, G_T{}^*(s)\} = \frac{r(s)H(e^{sT})}{2(b-z_a)+r(s)H(s))} \tag{34}$$

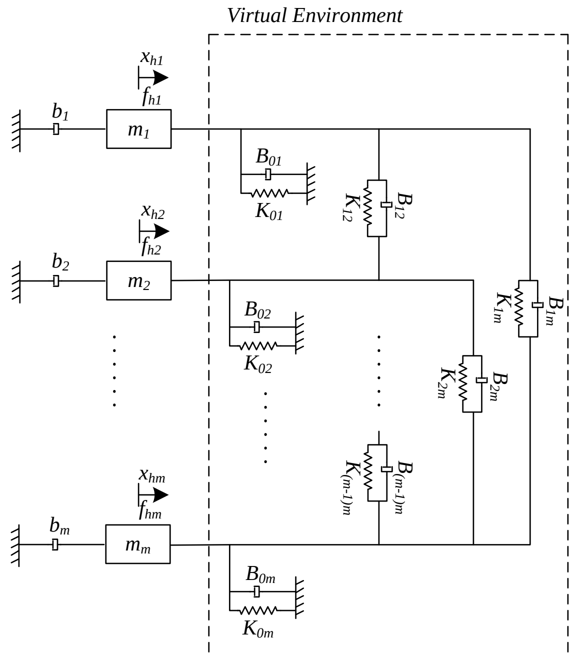

Figure 6: An m-user HVE system

Since, $\mathscr{M}$ is already in the unit disk, by applying small-gain theorem the condition for stability of the delayed single-user HVE system with active operator will be

$$\left|\frac{r(j\omega)H(e^(j\omega T)}{2(b-z_a)+r(j\omega)H(e^{j\omega T})}\right| < 1 \tag{35}$$

Straightforward manipulation then leads to the following condition:

$$b - z_a > \frac{T}{2}\frac{1}{1-\cos(\omega T)}\Re\{e^{-j\omega t_d}(1-e^{-j\omega T})H(e^{j\omega T})\} \tag{36}$$

For the virtual wall $H(z) = K + B\frac{z-1}{Tz}$ and assuming that B is small enough, this stability condition will again reduce to (27), where if $z_a = 0$ the condition will be identical to that reported in [7].

3.2 A Sampled-Data Multi-User HVE System

Based on the sampled-data single-user HVE system modeled in Figure 2, the model of a multi-user system can be presented as in Figure 6. Since each operator affects one master device only, the block diagram of the multi-user system can be modified to Figure 7a. A slight manipulation in Figure 7a will result in Figure 7b without affecting the overall system. The dynamics of the system in Figure 7b are as

$$b_i V_{hi}(z) = F_{hi}(z) - U_i(z), \quad i = 1, \cdots, m \tag{37}$$

where $V_{hi}(z) = \mathscr{Z}\{v_{hi}\}$, $F_{hi}(z) = \mathscr{Z}\{f_{hi}\}$, $U_i(z) = \mathscr{Z}\{u_i\}$. Note that

$$U(z) = z^{-n_i}H(z)X_h(z)$$

where $n_i = t_{di}/T$ is an integer and

$$H_{ii}(z) = K_{0i} + \Sigma_{k=1,k\neq i}^{m}(K_{ik} + \frac{(B_{0i}+\Sigma_{k=1,k\neq i}^{m}B_{ik})(z-1)}{Tz})$$

$$H_{ij}(z) = -(K_{ij} + \frac{B_{ij}(z-1)}{Tz}), \quad j \neq i$$

As a result, we have

$$U_i(z) = (K_{0i} + \Sigma_{k=1,k\neq i}^{m}K_{ik} + \frac{(B_{0i}+\Sigma_{k=1,k\neq i}^{m}B_{ik})(z-1)}{Tz})X_{hi}(z) - \Sigma_{j=1,j\neq i}^{m}(K_{ij} + \frac{B_{ij}(z-1)}{Tz})X_{hj}(z)$$

Substituting the forward difference approximation for $\frac{1}{s}$ in (38) and then combining the result with (37), the relationship between the force vector F_h and the velocity vector V_h can be written as

$$F_h(z) = G^{-1}(z)V_h(z) \tag{38}$$

where $G(z)$ is the $m \times m$ transfer matrix of the multi-user system. Again, we distinguish the following four cases.

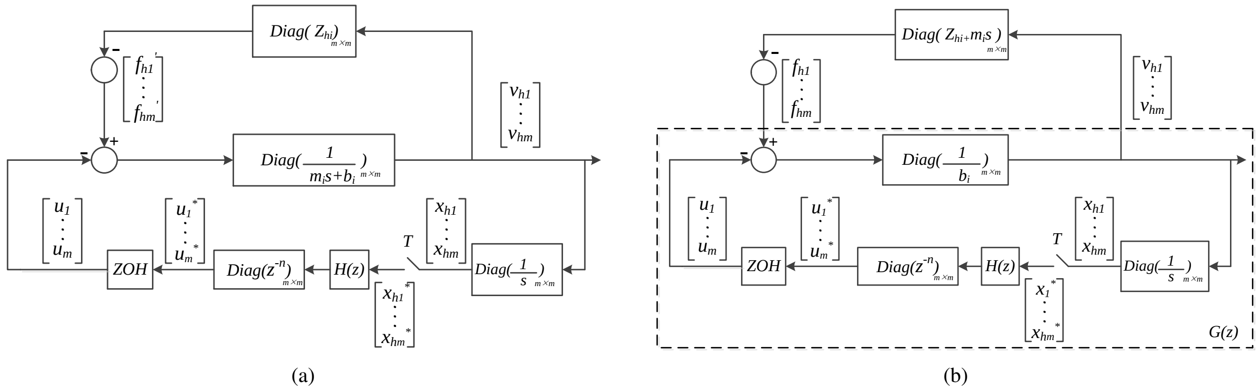

Figure 7: Model of a 1-DOF multi-user HVE system

Passive Operators No Delay Similar to the single-user case, Theorem 2.1 and Lemma 1 require the positive realness of $G^{-1}(z)$. Since the expression for $G(z)$ is involved for a general m-user system, let us begin by considering the special case of $m = 2$, for which

$$G^{-1}(z) = \begin{bmatrix} b_1 + \frac{(K_{01}+K_{12})T}{z-1} + \frac{(B_{01}+B_{12})}{z} & -(\frac{K_{12}T}{z-1} + \frac{B_{12}}{z}) \\ -(\frac{K_{12}T}{z-1} + \frac{B_12}{z}) & b_2 + \frac{(K_{02}+K_{12})T}{z-1} + \frac{(B_{02}+B_{12}}{z} \end{bmatrix} \tag{39}$$

With the first condition in Definition 2 being readily satisfied, the third condition in Definition 2 for positive realness of $G^{-1}(z)$ requires the poles on the $|z|= 1$ to be simple and have positive semidefinite residue matrices. As it can be clearly seen in (39), $z = 1$ is a simple pole and the residue matrix for this pole is

$$R_0 = \begin{bmatrix} (K_{01}+K_{12})T & -K_{12}T \\ -K_{12}T & (K_{02}+K_{12})T \end{bmatrix} \tag{40}$$

As it can be seen R_0 is a Hermitian matrix and based on Definition 3 it is positive semidefinite since

$$(K_{01}+K_{12})T > 0 \tag{41}$$

$$det(R_0) = (K_{01}K_{02} + (K_{01}+K_{02})K_{12})T^2 > 0 \tag{42}$$

Substituting $z = e^{j\omega T} = \cos(\omega T) + j\sin(\omega T)$, the second condition in Definition 2 for positive realness of $G^{-1}(z)$ will lead to the following two conditions:

$$b_1 - \frac{(K_{01}+K_{12})T}{2} + (B_{01}+B_{12})\cos(\omega T) > 0 \tag{43}$$

$$\begin{aligned} & det(G(e^{j\omega T}) + G^T(e^{-j\omega T})) = \\ & (2b_1 - K_{01}T + 2B_{01}\cos(\omega T))(2b_2 - K_{02}T + 2B_{02}\cos(\omega T)) \\ & + ((2b_1+2b_2) - (K_{01}+K_{02})T + 2(B_{01}+B_{02})\cos(\omega T)) \\ & (-K_{12}T + 2B_{12}\cos(\omega T)) > 0 \end{aligned} \tag{44}$$

The worst-case for (43)-(44) occurs when $\cos(\omega T) = -1$. With $b = \min(b_1, b_2)$, $B_0 = \max(B_{01}, B_{02})$ and $K_0 = \min(K_{01}, K_{02})$, the above two conditions will hold if

$$(2b - K_0T - 2B_0)^2 + 2(2b - K_0T - 2B_0)(-K_{12}T - 2B_{12}) > 0 \tag{45}$$

After simplifying (45), the stability condition for this sampled-data, dual-user HVE system will be

$$b > \frac{K_0T}{2} + K_{12}T + B_0 + 2B_{12} \tag{46}$$

Having found the stability condition for $m = 2$, let us know proceed to the case of $m = 3$. The matrix $G^{-1}(z)$ for the corresponding sampled-data, triple-user HVE system is

$$G^{-1}(z) = \begin{bmatrix} b_1 + \frac{K_1T}{z-1} + \frac{B_1}{z} & -(\frac{K_{12}T}{z-1} + \frac{B_{12}}{z}) & -(\frac{K_{13}T}{z-1} + \frac{B_{13}}{z}) \\ -(\frac{K_{12}T}{z-1} + \frac{B_{12}}{z}) & b_2 + \frac{K_2T}{z-1} + \frac{B_2}{z} & -(\frac{K_{23}T}{z-1} + \frac{B_{23}}{z}) \\ -(\frac{K_{13}T}{z-1} + \frac{B_{13}}{z}) & -(\frac{K_{23}T}{z-1} + \frac{B_{23}}{z}) & b_3 + \frac{K_3T}{z-1} + \frac{B_3}{z} \end{bmatrix}$$

where $K_1 = K_{01}+K_{12}+K_{13}$, $K_2 = K_{02}+k_{12}+K_{23}$, $K_3 = K_{03}+k_{13}+K_{23}$, $B_1 = B_{01}+B_{12}+B_{13}$, $B_2 = B_{02}+B_{12}+B_{23}$ and $B_3 = B_{03}+B_{13}+B_{23}$. Again, $G^{-1}(z)$ needs to be positive real. With all the poles of $G(z)^{-1}$ being on or inside the unit circle and applying the third condition in Definition 2, it can clearly be seen in (47) that $z=1$ is a simple pole and the residue matrix for this pole is

$$R_0 = \begin{bmatrix} (K_{01}+K_{12}+K_{13})T & -K_{12}T & -K_{13} \\ -K_{12}T & (K_{02}+K_{12}+K_{23})T & \\ -K_{13}T & -K_{23}T & (K_{03}+K_{13}+K_{23}) \end{bmatrix} \tag{47}$$

R_0 is a Hermitian matrix and based on Definition 3 it is positive semidefinite since

$$(K_{01}+K_{12}+K_{13})T > 0 \tag{48}$$

$$((K_{01}+K_{13})(K_{02}+K_{23})+K_{12}(K_{01}+K_{02}+K_{13}+K_{23}))T^2 > 0 \tag{49}$$

$$\begin{aligned} det(R_0) &= K_{01}K_{02}K_{03}+(K_{01}+K_{02}+K_{03})(K_{12}K_{13}+K_{12}K_{23}+K_{13}K_{23}) \\ &+K_{01}K_{02}(K_{13}+K_{23})+K_{01}K_{03}(K_{12}+K_{23})+K_{02}K_{03}(K_{12}+K_{13}) > 0 \end{aligned}$$

Substituting $z = e^{j\omega T} = \cos(\omega T) + j\sin(\omega T)$, the second condition in Definition 2 for positive realness of $G^{-1}(z)$ will lead to the following conditions:

$$b_1 - \frac{(K_{01}+K_{12}+K_{13})T}{2} + (B_{01}+B_{12}+B_{13})\cos(\omega T) > 0 \tag{50}$$

$$\begin{aligned} & det(G(e^{j\omega T})+G^T(e^{-j\omega T})) = \\ & (2b_1-(K_{01}+K_{12}+K_{13})T+2(B_{01}+B_{12}+B_{13})\cos(\omega T))(2b_2-(K_{02}+K_{12}+K_{23})T+2(B_{02}+B_{12}+B_{23})\cos(\omega T)) \\ & (2b_3-(K_{03}+K_{13}+K_{23})T+2(B_{03}+B_{13}+B_{23})\cos(\omega T))-2(K_{12}T+2B_{12})(K_{13}T+2B_{13})(K_{23}T+2B_{23})- \\ & (2b_1-(K_{01}+K_{12}+K_{13})T+2(B_{01}+B_{12}+B_{13})\cos(\omega T))(K_{23}T+2B_{23})^2-(2b_2-(K_{02}+K_{12}+K_{23})T+2(B_{02} \\ & +B_{12}+B_{23})\cos(\omega T))(K_{13}T+2B_{13})^2-(2b_3-(K_{03}+K_{13}+K_{23})T-2(B_{03}+B_{13}+B_{23})\cos(\omega T))(K_{12}T+2B_{12})^2 > 0 \end{aligned} \tag{51}$$

The worst-case for the above conditions occurs when $\cos(\omega T) = -1$. With $B = \min(B_{12}, B_{13}, B_{23})$, $B_0 = \max(B_{01}, B_{02}, B_{03})$, $K_0 = \min(K_{01}, K_{02}, K_{03})$, $K = \min(K_{12}, K_{13}, K_{23})$ and $b = \min(b_1, b_2, b_3)$, the above two conditions will hold if

$$(2b-K_0T-2B_0-4B)^3-2(KT+2B)^3-3(KT+2B)^2(2b-K_0T-2B_0-4B) > 0 \tag{52}$$

After simplifying (52), the stability condition for this sampled-data, triple-user HVE system will be

$$b > \frac{K_0T}{2}+\frac{3KT}{2}+B_0+3B \tag{53}$$

In a similar way, it is possible to show that the stability condition for any m will be

$$\min_i b_i > \max_i\{\frac{K_{0i}T}{2}+B_{0i}\}+m\max_{i,j\neq i}\{\frac{K_{ij}T}{2}+B_{ij}\} \tag{54}$$

As it can be seen from (54), when only one user is involved, the condition will reduce to Colgate's condition for sampled-data, single-user HVE system.

Active Operators, No Delay The above method also allows us to inspect the system stability in the presence of active operators. This is a marked advantage over the method in [3], which leads to involved equations when there is more than one user in the system making it very difficult to derive the stability conditions for active operators. But here, the circle criterion based method enables us to readily account for active operators. Assuming that operator Z_{hi} has shortage of passivity of z_{ai}, the stability condition in (54) will change into

$$\min_i\{b_i - z_{ai}\} > \max_i\{\frac{K_{0i}T}{2}+B_{0i}\}+m\max_{i,j}\{\frac{K_{ij}T}{2}+B_{ij}\} \tag{55}$$

The above condition can be derived in a manner similar to (26), so the details are not shown. Again, for only one operator, (55) will reduce to (26).

Passive Operators and Delay For a delayed m-user HVE system, assuming that $t_{di}/T = n_i$ is an integer and B_{0i} and B_{ij} are small enough, the stability condition will be derived below. Again, for simplicity, let us start with the special case of $m=2$. The matrix $G^{-1}(z)$ for the corresponding sampled-data, dual-user HVE system is

$$G^{-1}(z) = \begin{bmatrix} b_1+z^{-n_1}(\frac{K_1T}{z-1}+\frac{B_1}{z}) & -z^{-n_1}(\frac{K_{12}T}{z-1}+\frac{B_{12}}{z}) \\ -z^{-n_2}(\frac{K_{12}T}{z-1}+\frac{B_{1}2}{z}) & b_2+z^{-n_2}(\frac{K_2T}{z-1}+\frac{B_2}{z}) \end{bmatrix} \tag{56}$$

where $K_1 = K_{01}+K_{12}$, $B_1 = B_{01}+B_{12}$, $K_2 = K_{02}+K_{12}$ and $B_2 = B_{02}+B_{12}$. As before, based on Theorem 2.1 and Lemma 1, we require $G^{-1}(z)$ to be positive real assuming that the operators are passive. It can be easily shown that the first and third condition in Definition 2 are satisfied, leaving us with the second condition. Substituting $z = e^{j\omega T} = \cos(\omega T) + j\sin(\omega T)$, the second condition in Definition 2 for positive realness of $G^{-1}(z)$ will lead to the following three conditions:

$$t_{d1} = t_{d2} \tag{57}$$

$$b_1 + (B_{01} + B_{12})\cos(\omega(t_d - T)) - \frac{(K_{01} + K_{12})T}{2}\cos(\omega t_d) - (K_{01} + K_{12})TS > 0 \tag{58}$$

$$\begin{aligned}
&det(G(e^{j\omega T}) + G^T(e^{-j\omega T})) = (b_1 + B_{01}\cos(\omega(t_d - T)) - \frac{K_{01}T}{2}\cos(\omega t_d) - K_{01}TS)(b_2 + B_{02}\cos(\omega(t_d - T)) \\
&- \frac{K_{02}T}{2}\cos(\omega t_d) - K_{02}TS) + (B_{12}\cos(\omega(t_d - T)) - \frac{K_{12}T}{2}\cos(\omega t_d) - K_{12}TS)(b_1 + B_{01}\cos(\omega(t_d - T)) \\
&- \frac{K_{01}T}{2}\cos(\omega t_d) - K_{01}TS) + (B_{12}\cos(\omega(t_d - T)) - \frac{K_{12}T}{2}\cos(\omega t_d) - K_{12}TS)(b_2 + B_{02}\cos(\omega(t_d - T)) \\
&- \frac{K_{02}T}{2}\cos(\omega t_d) - K_{02}TS) > 0
\end{aligned} \tag{59}$$

where $S = \frac{\sin(\omega t_d)\sin(\omega T)}{2(1-\cos(\omega T))}$. As it can be seen from the first condition, $t_{d1} = t_{d2}$ (which in general will be $t_{di} = t_d$), the limitation of this method is that it cannot allow for different delay values in the multi-user architecture. Assuming that $t_d/T = n$ is an integer and B_{0i} and B_{ij} are sufficiently small and with $b = \min(b_1, b_2)$, $B_0 = \min(B_{01}, B_{02})$, and $K_0 = \max(K_{01}, K_{02})$ the worst-case for (57) and (59) occurs when S has its maximum value. Therefore, solving the $\frac{d}{d\omega}S = 0$ will lead us to $cos(\omega T) = 1$, which is confirmed to give the maximum value of S by checking the sign of the second derivative of S for $cos(\omega T) = 1$. The maximum value of S will then be

$$\lim_{\cos(\omega T)\to 1} \frac{\sin(\omega t_d)\sin(\omega T)}{2(1-\cos(\omega T))} = \frac{t_d}{T}$$

Then,

$$\begin{aligned}
&det(G(e^{j\omega T}) + G^T(e^{-j\omega T})) = \\
&(2b + 2B_0 + 2B_{12} - (K_{01} + K_{12})T - 2(K_0 + K_{12})t_d)^2 - (2B_{12} - K_{12}T - 2K_{12}t_d)^2 > 0
\end{aligned} \tag{60}$$

Simplifying (60) will give us

$$b + B_0 + 2B_{12} > \frac{K_0 T}{2} + K_{12}T + K_0 t_d + 2K_{12}t_d \tag{61}$$

In a similar way, the stability condition for a delayed m-user HVE system will be

$$\min_i\{b_i + B_{0i}\} + m\min_{i,j\neq i} B_{ij} > \max_i\{K_{0i}t_d + \frac{K_{0i}T}{2}\} + m\max_{i,j\neq i}\{K_{ij}t_d + \frac{K_{ij}T}{2}\} \tag{62}$$

Again, for a single-user system, condition (62) will reduce to (27).

Active Operators, Delay   Finally, with the addition of active operators to the delayed system and assuming that $t_d/T = n$ is an integer and B_{0i} and B_{ij} are small enough, the stability condition will be

$$\min_i\{b_i - z_{ai} + B_{0i}\} + m\min_{i,j\neq i} B_{ij} > \max_i\{K_{0i}t_d + \frac{K_{0i}T}{2}\} + m\max_{i,j\neq i}\{K_{ij}t_d + \frac{K_{ij}T}{2}\} \tag{63}$$

4 Simulation Study

In this section, the conditions derived throughout the paper are tested using MATLAB/Simulink. Since having an operator with a desirable amount of shortage of passivity is quite difficult to robustly implement in practice, experimental results will not be provided for conditions that allow operator activity; instead, such cases are tested in simulations. This is the main reason for reporting both simulations and experiments in this paper.

In order to test conditions (26) and (27), the sampled-data single-user HVE system in Figure 4a is simulated in MATLAB/Simulink. To determine the stability of the system, the system outputs are monitored for boundedness at all times -- if any output goes unbounded, the system is unstable.

For the non-delayed single-user HVE system with $m = 0.015$, $b = 0.02$ and $B = 0$, simulations have been conducted for three cases where the shortage of passivity z_a of the operator is either 0, $0.5b$, or $0.8b$. To this end, the operator model was considered to be $-z_a + \frac{1}{s}$; note that $\Re\{\frac{1}{s}\} = 0$ makes it a least-passive operator corresponding to a worst-case scenario for the coupled system stability.

During the simulations, the sampling time is increased by steps of $1ms$. For each sampling time, the controller gain K is changed to find the largest gain value for which the system remains stable. In Figure 8a, each of these maximum controller gain values at a given sampling period is represented by a star. Evidently, these simulation data points are very close to the solid lines, which correspond to the theoretical borderline given by (26). Therefore, the simulations confirm the theoretical condition (26). Also, as expected from (26), an increase in the shortage of passivity z_a will cause the stable region to shrink.

For the delayed single-user HVE system with $m = 0.15$, $b = 0.2$ and $B = 0$, the delay t_d is set to $10T$ and again simulations are conducted for the three cases involving shortages of passivity z_a of 0, $0.2b$, and $0.5b$. The simulation procedure is the same as before. As shown

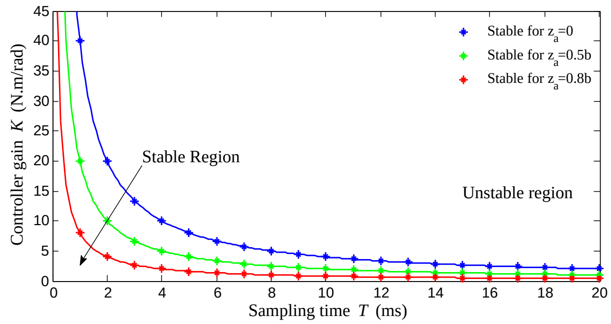

(a)

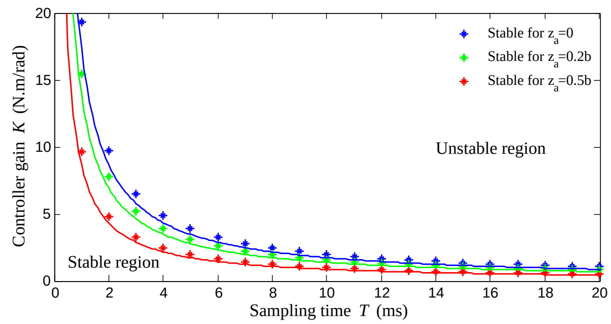

(b)

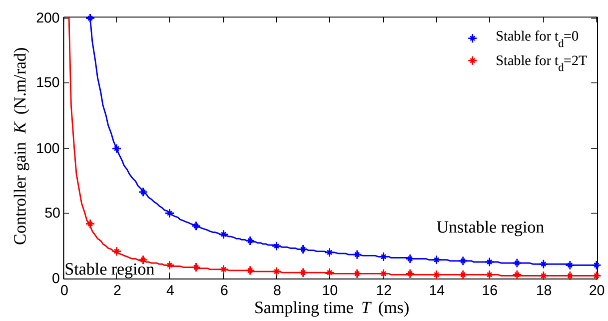

(c)

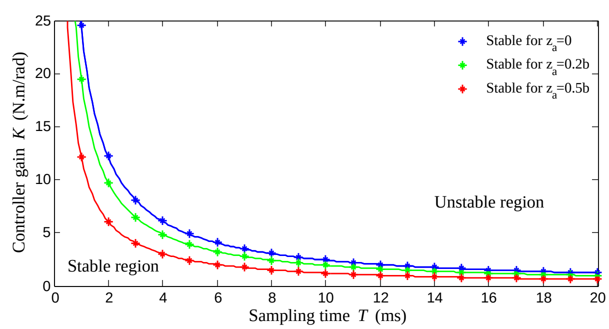

(d)

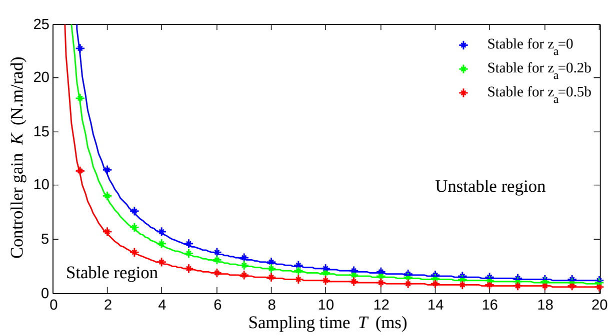

(e)

Figure 8: Simulation data points and corresponding theoretical borderlines for (a) a no-delay single-user HVE system, (b) a delayed ($t_d = 10T$), (c) non-delayed (blue) and delayed (red) single-user HVE system when the operator is allowed to have $z_a = 0.5b$ shortage of passivity, (d) a no-delay dual-user HVE system , and (e) a delayed ($t_d = 5T$) dual-user HVE system.

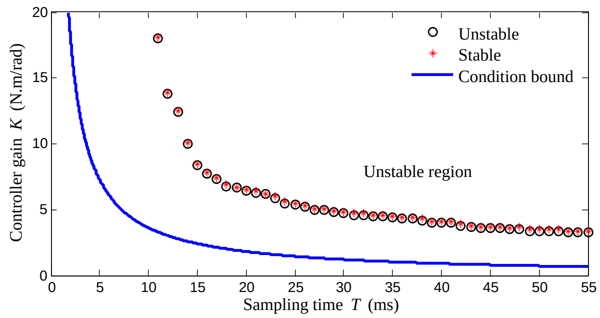

(a)

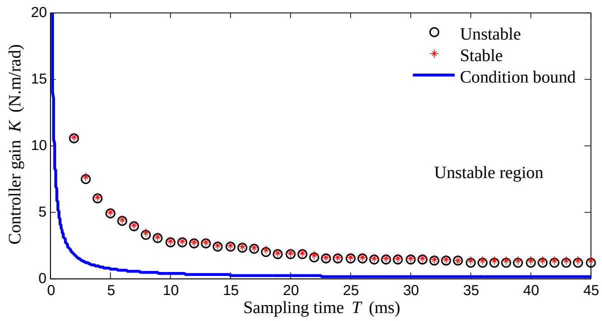

(b)

Figure 9: Experimental data points and theoretical borderlines for (a) a non-delayed single-user HVE system, and (b) a delayed ($t_d = 10T$) single-user HVE system

in Figure 8b, again the simulation data points represented by stars are close to the theoretical borderline (27). This time, there is a small gap between the simulation data points and the theoretical borderline, which corresponds to cases where condition (27) is conservative for detecting the system instability. The conservatism of condition (27) was predictable due to the fact that it was found as a sufficient condition for stability. Also, as before, any increase in the shortage of passivity z_a decreases the stability region as predicted by the theoretical condition (27).

It is also educational to compare the stability regions for a single-user HVE system with and without the time delay. As shown in Figure 8c, for the same shortage of passivity of the operator, delay causes the stability region to shrink. This was predictable if one compares the theoretical conditions (26) and (27) for $B = 0$.

Similar simulations are conducted for a sampled-data dual-user HVE system. Using MATLAB/Simulink the system in Figure 7a is simulated and conditions (55) and (63) are tested for $m = 2$. The simulations for both non-delayed dual-user HVE system with environment parameters $K_{01} = K_{02} = K_{12} = \frac{K}{2}$, $B_{01} = B_{02} = B_{12} = 0$, $m_1 = m_2 = 0.015$, and $b_1 = b_2 = 0.01822$ and delayed dual-user HVE system ($t_d = 5T$) with $K_{01} = K_{02} = K_{12} = \frac{K}{2}$, $B_{01} = B_{02} = B_{12} = 0$, $m_1 = m_2 = 0.15$, and $b_1 = b_2 = 0.1822$, are done for three cases with shortages of passivity z_a of 0, $0.2b$, and $0.5b$ (See Figures 8d and 8e). As before, there is a good match between the simulation results and the theoretically-derived stability borderlines.

5 Experimental Results

To verify the stability conditions (20) and (25), experiments involving a single-user HVE system consisting of a Phantom Premium 1.5A robot (Geomagic, Wilmington, MA) with a JR3 force sensor (JR3, Inc., Woodland, CA) at its end-effector are conducted. The mass and damping for the Phantom Premium 1.5A robot are $m = 0.015$ and $b = 0.01822$, respectively. The robot can move in three Cartesian directions and can be modeled as first-order transfer functions from the end-effector force input to the end-effector velocity output along each of these directions. Out of the three Cartesian axes, the x axis is used in the experiment while the y and z axes are locked using high-gain controllers. In agreement with the literature, the virtual environment composed of a spring and a damper in parallel as in Figure 2 has been implemented in discrete-time using the backward-difference method.

In the experiments, the robot is initially in free space and at some distance (initial condition) from the virtual wall. The initial condition is the difference in the position of the robot from its rest position, which is chosen to be co-located with the wall edge. Since a passive system should remain stable regardless of its initial condition, when investigating the stability of the system, the initial condition has been changed over a series of trials in a large span only limited by the physical constraints of the experimental setup. If the system becomes unstable in one trial (corresponding to a particular initial condition), it can be indicated that the system with the chosen parameters is unstable. If in none of the trials of an experiment with the controller gain K and the sampling time T the system becomes unstable, then it is identified as stable.

The procedure for experimentally determining the stability/instability borderline is as follows. The objective of the experiment is to determine the largest and smallest values of the controller gain K with which the system is stable and unstable, respectively. At different sampling times apart by steps of $1ms$ in a given range, the controller gain is altered gradually until the above-mentioned maximum and minimum gains are found. The exact experimental protocol for this process of changing the controller gain is described below. Starting with a value of K close to the value obtained from conditions (20) and (25) for a given sampling time T, if no instability is seen, the experiment is repeated with a larger initial condition while keeping the same controller gain K. If the system stays stable for all initial conditions tested in the robot workspace, the corresponding data point is considered as being stable in the $K-T$ plane. Then, K is increased (by steps of 0.1) and the previous procedure involving changing the robot initial condition is repeated. Increasing the value of K is continued until the system becomes unstable. The last data point for which the system is stable is marked as stable (represented by a star) in the $K-T$ plane. Also, the data point corresponding to the unstable experiment with the smallest controller gain K is marked by a circle in the $K-T$ plane.

The results of the above procedure form a stability borderline in the $K-T$ plane. The experimentally-obtained borderlines found for the non-delayed and delayed single-user HVE system with a passive operator are shown in Figure 9a and 9b, respectively. For each case, the theoretical regions of stability and instability obtained from conditions (20) and (25) are separated by the theoretical borderline (blue line). As explained before, the result of each experiment is indicated either as a star or a circle, which correspond to largest and the smallest controller gains for which the system will be stable or unstable, respectively. Note that for each sampling time, many more tests were conducted but they are not shown in Figures 9a and 9b; only those data points corresponding to the smallest and largest controller gains for unstable and stable systems are shown. From both Figures 9a and 9b, it is seen that the theoretical absolutely stable/potentially unstable borderline is more conservative than the experimentally-obtained borderline.

6 Conclusion

This paper studied the absolute stability of an m-user haptic virtual environment system based on the discrete-time circle criterion. In practice, depending on the task being performed by the human operator, the operator might behave passively or actively. The proposed stability analysis method enables a unified framework in which the human operators can demonstrate active or passive behavior. The same unified framework can be applied to study the stability with or without time delay. Simulation results and experiments confirm the validity of the proposed stability conditions.

References

[1] Gillespie RB, Cutkosky M. Stable user-specific rendering of the virtual wall. In: Proceedings of the ASME International Mechanical Engineering Conference and Exposition. vol. 58. Atlanta, GA; 1996. p. 397–406.

[2] Minsky M, Ming Oy, Steele O, Brooks FP Jr, Behensky M. Feeling and seeing: Issues in force display. In: Proceedings of the 1990 Symposium on Interactive 3D Graphics. I3D '90. New York, NY, USA: ACM; 1990. p. 235–241. Available from: http://doi.acm.org/10.1145/91385.91451.

[3] Colgate JE, Schenkel G. Passivity of a class of sampled-data Systems: Application to haptic interfaces. Journal of Robotic Systems. 1997;14(1):37–47.

[4] Gil JJ, Avello A, Rubio A, Florez J. Stability analysis of a 1 DOF haptic interface using the Routh-Hurwitz criterion. IEEE Transactions on Control Systems Technology. 2004 July;12(4):583–588.

[5] Hulin T, Preusche C, Hirzinger G. Stability boundary for haptic rendering: Influence of human operator. In: Intelligent Robots and Systems, 2008. IROS 2008. IEEE/RSJ International Conference on; 2008. p. 3483–3488.

[6] Tavakoli M, Aziminejad A, Patel RV, Moallem M. Discrete-time bilateral teleoperation: modelling and stability analysis. Control Theory and Applications, IET. 2008 June;2(6):496–512.

[7] Gil JJ, Sanchez E, Hulin T, Preusche C, Hirzinger G. Stability boundary for haptic rendering: Influence of damping and delay. Computing and Information Science in Engineering. 2009;.

[8] Dyck M, Jazayeri A, Tavakoli M. Is the human operator in a teleoperation system passive? In: World Haptics Conference (WHC), 2013; 2013. p. 683–688.

[9] Dela Sen A, Ibeas M, Alonso-Quesada S. Asymptotic hyperstability of a class of linear systems under impulsive controls subject to an integral Popovian constraint. In: Abstract and Applied Analysis; 2013. p. 14 pages. Available from: http://dx.doi.org/10.1155/2013/382762.

[10] Li R, Liu B, Liu C. Absolute stability and master-slave synchron ization of systems with state-dependent nonlinearities. In: Mathematical Problems in Engineering; 2013. p. 6 pages. Available from: http://dx.doi.org/10.1155/2013/326560.

[11] Basdogan C, De S, Kim J, Muniyandi M, Kim H, Srinivasan MA. Haptics in minimally invasive surgical simulation and training. Computer Graphics and Applications, IEEE. 2004;24(2):56–64.

[12] Chebbi B, Lazaroff D, Bogsany F, Liu PX, Niy L, Rossi M. Design and implementation of a collaborative virtual haptic surgical training system. In: Mechatronics and Automation, 2005 IEEE International Conference. vol. 1; 2005. p. 315–320 Vol. 1.

[13] Carignan CR, Olsson PA. Cooperative control of virtual objects over the Internet using force-reflecting master arms. In: Robotics and Automation, 2004. Proceedings. ICRA '04. 2004 IEEE International Conference on. vol. 2; 2004. p. 1221–1226 Vol.2.

[14] Carignan CR, Krebs HI. Telerehabilitation robotics: bright lights, big future? Journal of Rehabilitation Research and Development;43(5):695–710.

[15] Johnson M, Loureiro RV, Harwin W. Collaborative tele-rehabilitation and robot-mediated therapy for stroke rehabilitation at home or clinic. Intelligent Service Robotics. 2008;1(2):109–121. Available from: http://dx.doi.org/10.1007/s11370-007-0010-3.

[16] Ho C, Basdogan C, Slater M, Durlach N, Srinivasan MA. An experiment on the influence of haptic communication on the sense of being together. In: In Proceedings of the British Telecom Workshop on Presence in Shared Virtual Environments. ACM Press; 1998. p. 525–532.

[17] Goncharenko I, Svinin M, Matsumoto S, Masui Y, Kanou Y, Hosoe S. Cooperative control with haptic visualization in shared virtual environments. In: Information Visualisation, 2004. IV 2004. Proceedings. Eighth International Conference on; 2004. p. 533–538.

[18] Khalil HK. Nonlinear systems. Prentice Hall; 2002. Available from: http://books.google.ca/books?id=t_d1QgAACAAJ.

[19] Callier FM. Dissipative systems analysis and control: Theory and applications (2nd Edition)-[Book review; B. Brogliato, R. Lozano, B. Maschke]. Automatic Control, IEEE Transactions on. 2007;52(7):1357–1358.

[20] Hill DJ, Moylan PJ. Stability results for nonlinear feedback systems. Automatica. 1977;13(4):377 – 382. Available from: http://www.sciencedirect.com/science/article/pii/0005109877900206.

[21] Hitz L, Anderson BD. Discrete positive-real functions and their application to system stability. Proceedings of the Institution of Electrical and Engineers. 1969;(1):153–155.

[22] Gil JJ, Sanchez E, Hulin T, Preusche C, Hirzinger G. Stability boundary for haptic rendering: Influence of damping and delay. In: IEEE International Conference on Robotics and Automation. Rome, Italy; 2007. p. 124–129.

[23] Astrom KJ, Wittenmark B. Adaptive control. 2nd ed. Boston, MA, USA: Addison-Wesley Longman Publishing Co., Inc.; 1994.